# The Fe2+–HisF8 Raman Band Shape of Deoxymyoglobin Reveals Taxonomic Conformational Substates of the Proximal Linkage

**ARTICLE** *in* BIOPHYSICAL JOURNAL · OCTOBER 2001

Impact Factor: 3.97 · DOI: 10.1016/S0006-3495(01)75816-X · Source: PubMed



**3 AUTHORS:**

Joachim Schott
Universität Bremen
**6** PUBLICATIONS **78** CITATIONS
SEE PROFILE

Dreybrodt Wolfgang
Universität Bremen
**194** PUBLICATIONS **4,757** CITATIONS
SEE PROFILE

Reinhard Schweitzer-Stenner
Drexel University
**218** PUBLICATIONS **4,316** CITATIONS
SEE PROFILE

# The $Fe^{2+}$-$His^{F8}$ Raman Band Shape of Deoxymyoglobin Reveals Taxonomic Conformational Substates of the Proximal Linkage

Joachim Schott,* Wolfgang Dreybrodt,* and Reinhard Schweitzer-Stenner†
*FB1-Institut für Experimentelle Physik, Universität Bremen, 28359 Bremen, Germany; and †Department of Chemistry, University of Puerto Rico, San Juan, Puerto Rico 00931 USA

ABSTRACT The band shape of the Raman line attributed to the $Fe^{2+}$-$N_\epsilon(His^{F8})$ stretching mode in deoxymyoglobin contains significant information on the nature of the Fe-His proximal linkage. Raman lines appearing close to it, however, obscure the true line profile. To isolate this from its accompanying lines we use its isotopic shift of ~1 $cm^{-1}$ when $^{56}Fe$ in natural-abundance deoxymyoglobin is substituted by $^{54}Fe$. This enables us to isolate the true line shape. We have measured this line shape in sperm whale myoglobin dissolved in a 66% vol/vol glycerol/water solution for nine temperatures from 10 K to 300 K. The $\nu$(Fe-His) band shows a complex temperature-dependent profile, with a shoulder on its high-frequency wing, which becomes more prominent with increasing temperature. Detailed analysis reveals that the band is composed of five distinct lines attributable to taxonomic conformational substates of the $\nu$(Fe-His) linkage. These are in thermodynamic equilibrium above the glass transition temperature $T_f$ but freeze in into the thermodynamic distribution at $T_f$ for lower temperatures. Alternative models that try to explain the $\nu$(Fe-His) band shape by either an anharmonic coupling of the $\nu$(Fe-His) to a low-frequency heme doming mode or by conformational substates related to a Gaussian distribution of iron out-of-plane displacements are at variance with the distinct features observed experimentally.

## INTRODUCTION

It is well recognized that the proximal $Fe^{2+}$-$N_\epsilon(His^{F8})$ linkage in heme proteins plays a pivotal role in communicating protein structural changes to the functional heme group, thus affecting its biological properties (Gellin et al., 1983). Twenty years ago, Kitagawa and co-workers (Kitagawa et al., 1979, Hori and Kitagawa, 1980; Kitagawa, 1988) showed that resonance Raman scattering of deoxyheme proteins contains a band in the region between 200 $cm^{-1}$ and 250 $cm^{-1}$ assignable to the $Fe^{2+}$-$N_\epsilon(His^{F8})$ stretching mode $\nu$(Fe-His). The intensity and frequency of this band was found to strongly depend on the tertiary and quaternary structure of the respective heme protein (Rousseau and Friedman, 1988). Hence, it became a prominent marker band in the investigation of the relationship between structure and function of this class of proteins.

A number of studies in our laboratory have shown that for some heme-proteins, the $\nu$(Fe-His) band profile is asymmetric depending on solvent conditions such as pH and temperature (Bosenbeck et al. 1992, Gilch et al., 1993, 1995, 1996). For myoglobin, the band profile is less asymmetric but also exhibits a significant dependence on temperature. All these findings were interpreted by Gilch et al. (1995, 1996) as resulting from taxonomic conformational substates (Frauenfelder et al., 1991) with different conformations of the heme-$His^{F8}$ complex. These substates could be of functional relevance because the association and dissociation of ligands to and from the heme iron depends on the metal displacement and the orientation of the proximal imidazole ring (Friedman, 1985)

This interpretation was recently challenged by Bitler and Stavrov (1999). They rationalized the temperature dependence of the $\nu$(Fe-His) band of horse heart myoglobin by invoking anharmonic coupling between $\nu$(Fe-His) and the heme doming mode at 60 $cm^{-1}$. The main effect of this mechanism is that it causes the energy difference between subsequent vibrational levels of $\nu$(Fe-His) to depend on the vibrational quantum number of the heme doming mode and thus on temperature. This is illustrated by Eq. 6 in Bitler and Stavrov (1999). It represents the energies of these vibrational levels ($N$, $n$):

$$E_{N,n} = \hbar\Omega_0\left(N+\frac{1}{2}\right) + \hbar\omega_0\left(n+\frac{1}{2}\right) - \frac{\xi}{2}\hbar\Omega_0\left(N+\frac{1}{2}\right)^2 \times\left[1+2\gamma\frac{\left(n+\frac{1}{2}\right)}{\left(N+\frac{1}{2}\right)}\right], \quad (1)$$

where

$$\xi = \frac{\hbar\Omega_0\alpha^2}{m\omega_0^2}; \quad \text{and} \quad \gamma = \frac{\omega_0}{2\Omega_0}\left(1-\frac{\beta}{\alpha^2}\right). \quad (2)$$

$N$, $n$, $\Omega_0$, and $\omega_0$ are the vibrational quantum numbers and the vibrational frequencies of the $\nu$(Fe-His) and heme doming oscillators, respectively. (By mistake, Stavrov and Bitler exchanged the labeling of these quantum numbers.) $\alpha$ and $\beta$ are anharmonic coupling parameters appearing in the higher-order expansion of the anharmonic potential. The fre-

*Received for publication 11 July 2000 and in final form 4 June 2001.*

Address reprint requests to Dr. Wolfgang Dreybrodt, FB1-Institut für Experimentelle Physik, Universität Bremen, Kufsteinerstrasse 1, 28359 Bremen, Germany. Tel.: 49-421-218-3556; Fax: 49-421-218-7318; E-mail:dreybrod@physik.uni-bremen.de.



0006-3495/01/09/1624/08 $2.00

quency of a Raman transition from ($N \rightarrow N+1$, $n \rightarrow n$) is therefore

$$\hbar\Omega_0^{\mathrm{N}} = \hbar\Omega_0\left(1 - \xi\left[1 + N + \gamma\left(n + \frac{1}{2}\right)\right]\right). \qquad (3)$$

Because $\xi$ is positive and $\gamma$ had been neglected in the further calculations by Bitler and Stavrov (1999), the energy difference between $N$ and $N+1$ levels of the $\nu$(Fe-His) modes decreases with increasing $N$. As a consequence, at high temperatures, Raman lines of the $\nu$(Fe-His) resulting from transitions from populated higher vibrational states, for example ($N = 1$, $n \rightarrow N = 2$, $n$), ($N = 2$, $n \rightarrow N = 3$, $n$), etc. appear at lower frequencies as that of the ($N = 0$, $n \rightarrow N = 1$, $n$) transition. Therefore the $\nu$(Fe-His) band exhibits an asymmetric broadening at its low-frequency wing. Upon lowering the temperature, the higher vibrational levels of the $\nu$(Fe-His) and the heme doming mode become less populated, and as a consequence, the asymmetry is reduced and the peak frequency of the $\nu$(Fe-His) band shifts to higher values. At $T = 0$ K only one line due to the ($N = 0$, $n \rightarrow N = 1$, $n$) transitions survives.

By employing this model, Bitler and Stavrov (1999) were able to fit six $\nu$(Fe-His) profiles measured at different temperatures between 10 K and 300 K for horse heart myoglobin in an aqueous/ice solvent by Gilch et al. (1995). To obtain satisfactory fits to all these data, however, they had to assume that the glass transition of the solvent changes the vibronic coupling strength and the intensity of the $\nu$(Fe-His) band and also the intensity of another yet unidentified band at 202 $\mathrm{cm}^{-1}$. The success of their fitting led Bitler and Stavrov (1999) to conclude that the anharmonic coupling model generally suffices to explain the temperature dependence and the high-temperature asymmetry of $\nu$(Fe-His) band, so that they consider it superfluous to invoke the presence of conformational substates.

Fitting this subtle line shape to the experimental data, however, is not without pitfalls. First, the $\nu$(Fe-His) line is accompanied by two strong lines, one at 202 $\mathrm{cm}^{-1}$ at its low-frequency wing and another one at 241 $\mathrm{cm}^{-1}$ on the other side. They both overlap the $\nu$(Fe-His) band considerably. Moreover, the signal-to-noise ratio was just ~8. Therefore, the true $\nu$(Fe-His) line shape shows up only in a narrow region close to its maximum, between ~215 $\mathrm{cm}^{-1}$ and 230 $\mathrm{cm}^{-1}$. To discriminate between the correctness of the fits to taxonomic sublines as suggested by Gilch et al. (1993, 1995) or the anharmonic coupling model of Bitler and Stavrov (1999) one therefore needs more accurate data, i.e., improvement of signal-to-noise ratio and elimination of overlapping Raman lines obscuring the $\nu$(Fe-His) band shape.

In the present study we remeasured Raman spectra of sperm whale deoxymyoglobin (deoxyMb) in a glycerol/water solution. Moreover, we recorded Raman spectra of deoxyMb with an isotopically labeled $^{54}$Fe heme group. This enabled us to isolate the $\nu$(Fe-His) band profile from the overlapping lines. By carefully preparing our samples to achieve an extremely low fluorescence background and by use of a CCD camera we were able to obtain an excellent signal-to-noise ratio of ~46. By these means we succeeded to isolate the $\nu$(Fe-His) band shape. Its analysis unequivocally reveals the existence of conformational heterogeneity of the $\nu$(Fe-His) linkage

## MATERIALS AND METHODS

In the past, Raman spectroscopy at low temperatures on heme proteins in glycerol/water mixtures was rendered difficult due to a disturbing fluorescence background. It generally is caused by unpolar fragments of myoglobin itself. Even small amounts can spoil Raman spectra. The fragments result from the lyophilized protein, microbiological activity, destruction by the freezing process, and microbubbles of gas in the solution. Especially oxygen has destructive forces.

For the preparation of our samples, we carried out the following procedure. All glass equipment used was autoclaved at 140°C. The glove box with all its equipment was cleaned with 70% alcohol and illuminated by an ultraviolet lamp mounted inside before preparation. It was filled with pure nitrogen of 5.9 quality. The buffer was freshly prepared as a mixture of 0.1 M potassium dihydrogen phosphate (pH 4.1) and 0.1 M potassium hyhdrogen phosphate (pH 9.1) to adjust the desired pH of 6.6. The buffer was degassed and autoclaved at temperatures of ~140°C. Glycerol was degassed for several hours because of its high viscosity. Native lyophilized sperm whale (sw) Mb was purchased from Sigma Chemical Co. (St. Louis, MO), and the swMb with $^{54}$Fe-labeled heme (lyophilized) was produced by a method described by Teale (1959) and obtained as a kind gift from Dr. A. Ostermann. (Physics Department, Technical University Munich, Munich, Germany). Four micromolar myoglobin (69 mg) was filled into a tube for centrifugation and was transferred into a glove box. In all following steps it was kept in a 1-bar $N_2$ atmosphere. Myoglobin was dissolved in 1.8 ml of 0.1 M buffer at pH 6.6. The metmyoglobin/buffer solution was centrifuged at 5900 $\times$ $g$ for 20 min. An aliquot of 0.9 ml was taken from the top of the sample and transferred into a second tube. Metmyoglobin was then reduced to deoxymyoglobin by adding 4 $\mu$M dithionite (0.696g) dissolved in a 0.1-ml buffer solution. After an additional centrifugation, the upper 0.5 ml was transferred into a third tube, and 1 ml glycerol was added to obtain a 66% vol/vol glycerol/buffer solution, with a final concentration of 0.67 mM myoglobin. The sample was stirred very gently until it was homogeneous and clear. No additional chemicals were added. The state of the sample was checked for concentration and oxygenation by absorption spectroscopy. The pH of all samples was found between 6.7 and 6.9. The part of the sample not used for the subsequent measurement was stored at −20°C in a refrigerator, and 150 $\mu$l of the Mb solution was filled into the sample holder shown schematically by Fig. 1. It consists of an inner vessel made of acryl with a V-shaped space of 300 $\mu$l, which is covered by an acryl window. This inner vessel was thermally coupled to an outside vessel consisting of oxygen-free copper. The entire unit was screwed to the cooling finger of the cryostat. The V-shaped space was filled half with the narrow part pointing downward. This setup was used to avoid internal strain in the frozen sample. Its status was checked by measuring the depolarization ratio of the $\nu_4$-Raman line at 1355 $\mathrm{cm}^{-1}$. At 10 K, the observed depolarization ratio was $\rho = 0.20$ with $\lambda = 442$-nm excitation. Because this compares reasonably well with the room temperature value of $\rho = 0.16$, we concluded that the sample is nearly free of strain. With an almost completely filled vessel, however, we observed a depolarization ratio of $\rho = 0.5$ at 10 K, indicating large depolarization due to internal strain.

To measure Raman spectra as a function of temperature we used a refrigerator cryostat RDK10–320 from Leybold (Cologne, Germany). This

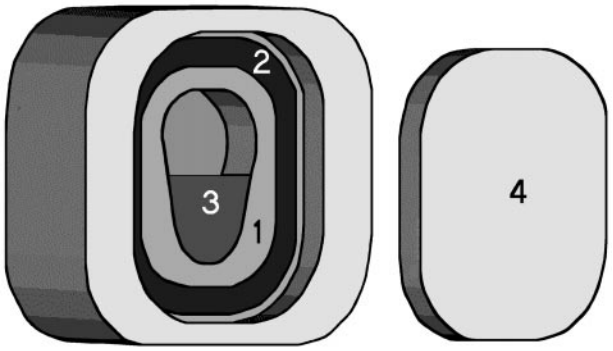


FIGURE 1 Sample holder: inner vessel (*1*) with O-ring (*2*), myoglobin solution (*3*), and lid (*4*)

cryostat has a programmable and computer-controlled temperature unit, which allows regulation of temperatures between 10 K and 320 K. In our standard protocol the sample was cooled down from 300 K to 10 K at a rate of 4 K/min. After thermal equilibration for 2 h, the first spectrum was measured. To control the quality of the sample we first measured the $\nu_4$ line at 1355 $cm^{-1}$ and subsequently the $\nu$(Fe-His) region. These two measurements were then repeated at various temperatures, which were adjusted by heating the sample at 4 K/min and by allowing a 1-h equilibration of the sample after the desired temperature was reached. In a second protocol, we measured a series of Raman spectra by cooling down from room temperature. Again, the system was allowed to equilibrate for a period of 1 h at each desired temperature. The two protocols yielded almost identical spectra at each of the adjusted temperatures. Spectra were obtained at 10, 50, 70, 100, 130, 165, 190, 230, and 270 K.

The Raman spectra of the $\nu$(Fe-His) band region were recorded by employing a conventional Raman spectrometer (Spex-1401, Spex Industries, Edison, NJ) with a resolution of 2.5 $cm^{-1}$. The exciting laser light of $\lambda = 441.6$ nm from a 30-mW He-Cd laser (Laser 2000, Munich, Germany) was polarized vertically and focused onto the sample by a 10-cm cylindrical lens. The scattered light was imaged onto the entrance slit of the double monochromator. A polarization scrambler was located close to the entrance slit. The light dispersed was detected by a CCD-camera (Photometrics, SDS9000, Tucson, AZ) with a back-illuminated chip from SITE (TK512CB). To calibrate the pixels versus wavenumber after each measured spectrum, a second spectrum was recorded by focusing stray light of xenon, krypton, or argon spectral lamps onto the entrance slit. A third spectrum was measured to determine the position of the laser frequency, which was stable within 0.1 $cm^{-1}$ during the time the spectra was taken, but on a time scale of hours showed variations of several $cm^{-1}$. By virtue of this procedure, a reproducibility of $\sim\pm 0.1$ $cm^{-1}$ was achieved for the frequency positions between 160 $cm^{-1}$ and 330 $cm^{-1}$. Finally, a complete heme spectrum between 160 $cm^{-1}$ and 1700 $cm^{-1}$ was recorded to check the status of the sample and to secure the critical issue of an individual-adapted, but consistent, determination of the baseline for all spectra measured. The baselines were subtracted before the analysis of the spectra, which were then calculated by means of our program MULTIFIT as a composition of single Gaussian lines (Unger et al., 1997). The Gaussian lines were convoluted with the slit function of the spectrometer and had fixed frequency positions and half-widths. The fit was performed simultaneously for the entire set of spectra obtained at nine different temperatures. Only the intensities of the composing lines were used as free fitting parameters. Such a self-consistent global fitting procedure secures an unambiguous fit to all spectra.

We like to emphasize that as stated earlier (Gilch et al., 1995) it is also possible to obtain satisfactory fits by use of Lorentzian sublines. For the higher-temperature region (270 K), however, the fits with Lorentzian lines proved to be inferior to those with Gaussian line shape. We therefore preferred the fits with Gaussians.

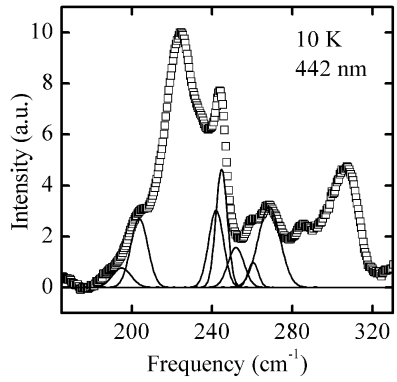


FIGURE 2 Raman spectrum in the low-frequency region for n.a. deoxymyoglobin. The separately drawn lines do not show frequency shifts compared with $^{54}$Fe-substituted myoglobin. The lines that compose the $\nu$(Fe-His)-band are identified by their frequency shifts in the $^{54}$Fe spectrum and are not shown here but are depicted in Fig. 6

## RESULTS AND DISCUSSION

### Isolation of the $\nu$(Fe-His) band profile

Fig. 2 shows the Raman spectrum of sw deoxyMb between 160 $cm^{-1}$ and 320 $cm^{-1}$. The very intense central band is assignable to $\nu$(Fe-His) and is overlapped on both sides by a variety of Raman lines resulting from other heme vibrations. They obscure the band shape of the $\nu$(Fe-His) mode and render an exact line shape analysis difficult. It cannot be excluded that the success of different approaches (Gilch et al., 1995, Bitler and Stavrov, 1999) in fitting the $\nu$(Fe-His) band shape heavily depended on how the authors separated it from the overlapping lines by their curve-fitting procedure.

To unambiguously identify the true band shape of $\nu$(Fe-His) we measured and compared the Raman spectra of the natural-abundance (n.a.) and of isotopically labeled $^{54}$Fe heme of sw deoxyMb. It is well known that $^{56}$Fe/$^{54}$Fe substitution causes an upshift of the $\nu$(Fe-His) frequency by $\sim 1$ $cm^{-1}$ (Kitagawa et al. 1979; Argade et al., 1984). This behavior was used to isolate the $\nu$(Fe-His) band shape from its overlapping lines as follows. We first analyzed the spectrum shown in Fig. 2 to resolve a variety of lines close to the wings of the $\nu$(Fe-His) band. All lines resulting from $\nu$(Fe-His) exhibit a frequency shift due to substitution with $^{54}$Fe, whereas all overlapping lines remain unaffected. Thus, by fitting the spectra of n.a. and $^{54}$Fe-labeled deoxyMb all non-$\nu$(Fe-His) lines were identified. By subtracting them from the observed spectra the $\nu$(Fe-His) band was isolated. The isolated band profile of n.a. myoglobin is shown in Fig. 3 for various temperatures. It exhibits a significant asymmetry and a temperature-dependent shift of its shape and frequency position. This was also observed for the isolated $\nu$(Fe-His) band of $^{54}$Fe-myoglobin.

The validity of the $\nu$(Fe-His) band isolation was verified after appropriate intensity scaling by shifting the profiles

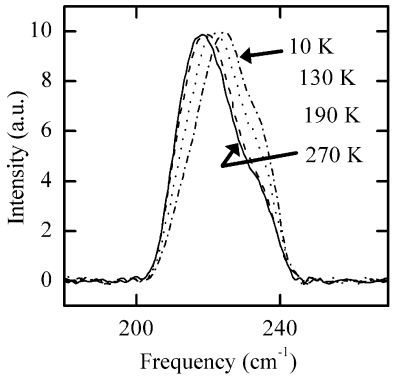


FIGURE 3 The band shape of the $\nu$(Fe-His) for n.a. deoxymyoglobin at various temperatures.

obtained for $^{54}$Fe-labeled deoxyMb onto the corresponding profile of the n.a. protein until their difference became minimal. Fig. 4 displays the overlaid spectra and their respective difference spectra for eight temperatures. The differences are within the noise of the measurement. The average value of the frequency shift from the $^{54}$Fe-heme to the n.a. spectra was determined to be $-1.1 \pm 0.2$ cm$^{-1}$, somewhat lower than observed earlier (Kitagawa et al., 1979; Argade et al., 1984).

## Application of the anharmonic coupling theory by Bitler and Stavrov

Both sets of profiles were now subjected to analyses by employing first the Bitler-Stavrov model (1999) and then the subline model proposed by Gilch et al. (1995). The anharmonic coupling approach of Bitler and Stavrov predicts a single Lorentzian line at 10 K, which results from a ($N = 0$; $n \rightarrow N = 1$; $n$) transition. When the temperature increases the ($N = 1, 2, \ldots$; $n$) states become more populated, and consequently, Raman lines due to ($N = 1, 2, \ldots$; $n \rightarrow N = 2, 3, \ldots$; $n$) transitions arise (cf. Eq. 3 with $\gamma = 0$). Their frequency is lower because of the anharmonic coupling, so that a skew asymmetry appears at the low-frequency side (cf. Fig. 3 in Bitler and Stavrov, 1999). As a consequence, the band maximum shifts to lower frequen-

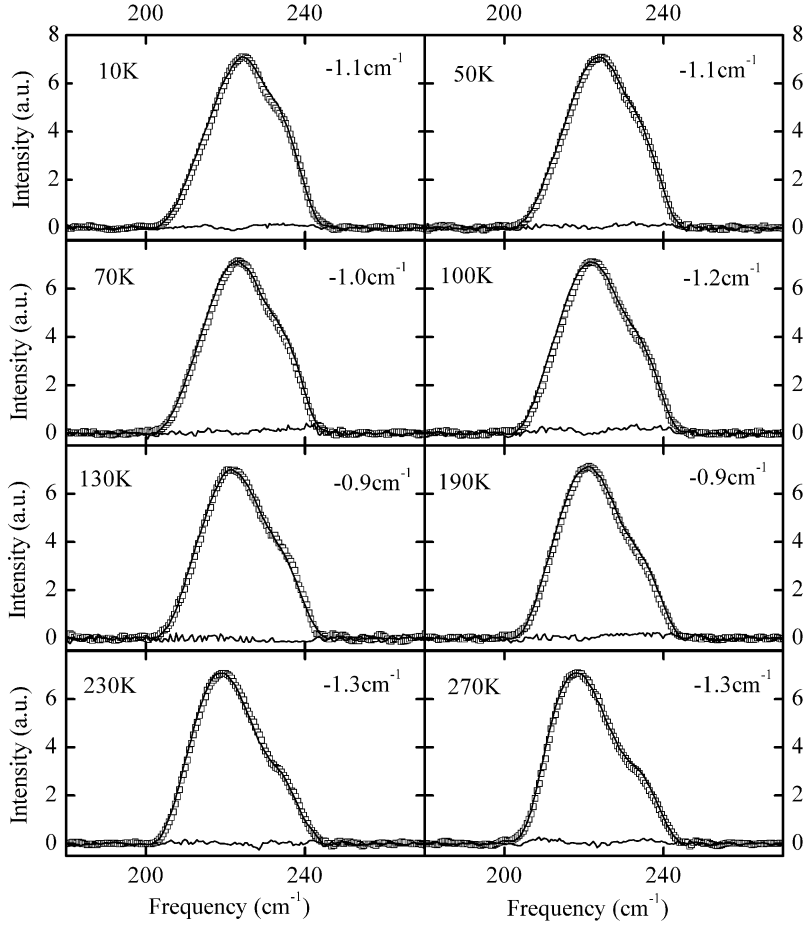


FIGURE 4 Isolated $\nu$(Fe-His) of $^{54}$Fe-myoglobin (—) shifted to overlay the isolated $\nu$(Fe-His) of n.a. myoglobin (□). The lower line depicts the difference of these spectra. The frequency shift is given in the right corner.

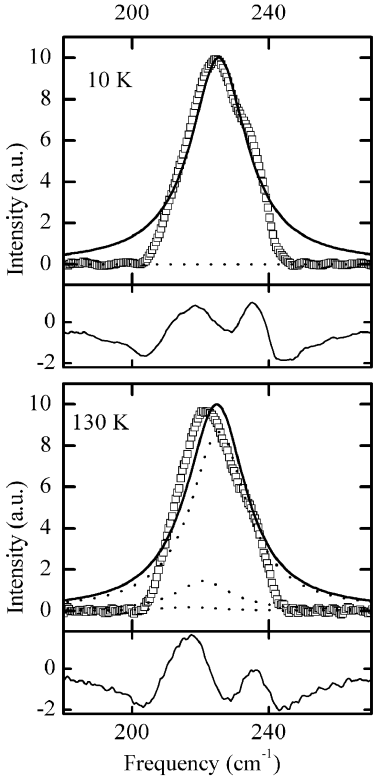


FIGURE 5 Best fit to the $\nu$(Fe-His) obtained with the model of Bitler and Stavrov (1999). The lower panels depict the difference between the measured data (□) an the fit (——). The dotted lines represent the single transitions adding up to the band profile.

cies. This behavior is in contrast to the observations shown in Fig. 3 in that the asymmetry clearly appears on the high-frequency side of the band at all temperatures investigated. This observation already qualitatively leads to the conclusion that the observed band profiles cannot be described by the Bitler and Stavrov theory.

This notion is confirmed by a direct, quantitative comparison. We first utilized their approach to fit the $\nu$(Fe-His) band measured at 10 K. As expected, this yields a single line. We used the frequency $\Omega_0$, the half-width $\Gamma_0$, and the intensity of the Lorentzian line as free parameters and inserted the coupling constant $\alpha = -0.9$ and the heme doming vibration $\omega_0 = 70\ \mathrm{cm}^{-1}$ to fit the $\nu$(Fe-His) band at 10 K. The best fit due to the $\chi^2$ test is shown in Fig. 5. Although a moderate agreement is achieved close to the maximum, we find large deviations in the wings of the band. Using the same parameters for fitting the $\nu$(Fe-His) profile measured at 130 K we obtained a second subline due to anharmonicity with an intensity of ~15% (Fig. 5), which, however, does by no means account for the experimentally observed shift of the peak frequency. Bitler and Stavrov (1999) obtained a much better agreement by fitting their model to the experimental data of Gilch et al. (1995). We believe that this stems from an overestimation of the contributions by overlapping side lines in their spectral analysis.

### Application of the substates model by Gilch et al.

The model of Gilch et al. (1995, 1996) assumed that the $\nu$(Fe-His) linkage exists in multiple but distinguishable taxonomic conformational substates that are in thermodynamic equilibrium. They give rise to sublines that constitute the $\nu$(Fe-His) band profile. This model resembles an approach commonly used for the analyses of the $\nu_{CO}$-IR band of MbCO and other heme proteins with the same ligand (Ansari et al., 1987; Iben et al., 1989; Braunstein et al., 1993). By using this model we self-consistently fitted the isolated band profiles by a common set of five sublines with fixed line positions and half-widths. The only free fitting parameters used were the line intensities. Fig. 6 shows four representative fits of the $\nu$(Fe-His). Their residuals displayed in the lower part of the panels are within the limits of noise. Fits of this quality were obtained independently for both n.a. and $^{56}$Fe-myoglobin at all temperatures measured. The frequencies of the sublines and their half-widths are listed in Table 1. According to the model of Gilch et al. (1995) the intensity ratios of sublines $i$ and $j$, respectively, are described as function of temperature by

$$R_{ij} = \frac{I_i}{I_j} = \exp\left(-\frac{\Delta H_{ij}}{RT_{eff}} + \frac{b_{ij}T_{eff}}{2R}\right)\exp\left(\frac{\Delta S_{ij}}{R}\right), \quad (4)$$

where $\Delta H_{ij}$ and $\Delta S_{ij}$ are the difference in enthalpy and entropy between the corresponding substates, respectively. $b_{ij}$ reflects differences in the first temperature derivative of their specific heat. $T_{eff}$ is an effective temperature that describes freezing into a glass-like state at temperature $T_f$:

$$T_{eff} = \frac{T}{1 + \exp\left(\frac{T_f - T}{\Delta T}\right)} + \frac{T_f}{1 + \exp\left(\frac{T - T_f}{\Delta T}\right)}. \quad (5)$$

Above $T_f$ the substates are in thermodynamic equilibrium, but below $T_f$ their motion freezes and their thermodynamic distribution is close to that at $T_f$.

In Fig. 7, $\ln(R_{ij})$ is plotted versus the reciprocal of the temperature $T$. The full lines represent a fit of Eqs. 4 and 5 to the experimental data. The fitting parameters are listed in Table 2. The temperature parameters obtained were $T_f = (150 \pm 8)$ K and $\Delta T = (98 \pm 8)$ K. The values of all fitting parameters, $\Delta H_{ij}$, $\Delta S_{ij}$, and $b_{ij}$, are close but not identical to those reported by Gilch et al. (1995). They fit well into the range expected for taxonomic conformational substates (cf. the detailed discussion in Gilch et al., 1995). The minor differences are not surprising because different solvents and proteins (sw Mb and horse heart Mb) were used. The transition temperature $T_f$ obtained is slightly lower than the glass temperature of the solvent, which is ~185 K for the glycerol/water mixture, but lies well within the broad tran-

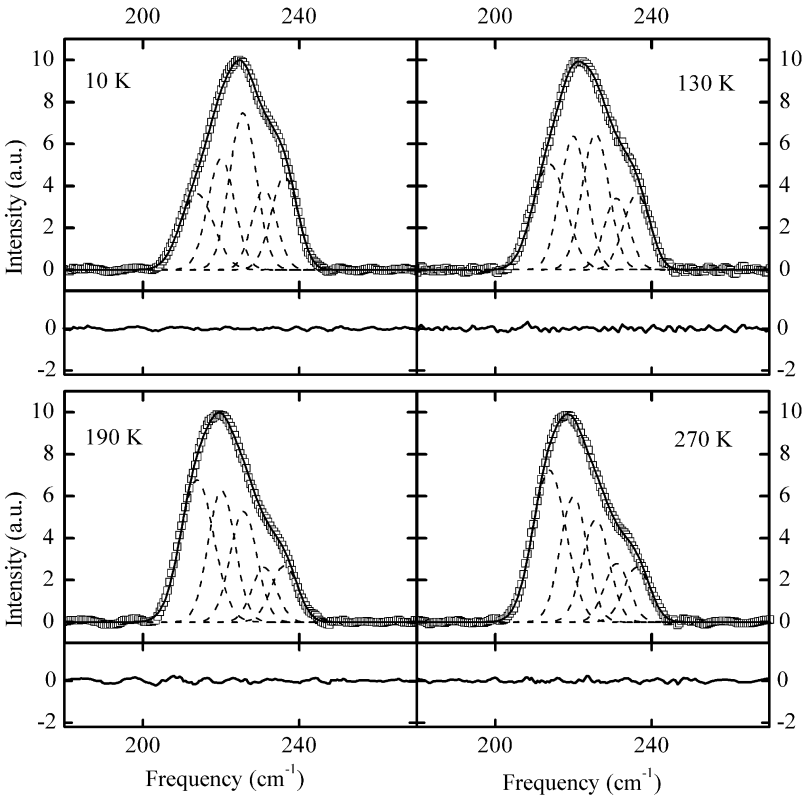


FIGURE 6 Fits obtained by assuming that all spectra, obtained at nine different temperatures (only four are shown here) consist of five distinct lines with varying intensities, which are used as fitting parameters. The lower panels depict the difference between experimental points (□) and fits (——). The dashed lines represent the five sublines.

sition region observed in other experiments e.g., infrared (Iben et al., 1989), neutron scattering (Doster et al., 1989), and Mössbauer experiments (Parak et al., 1982) on myoglobin. This indicates that the $\nu$(Fe-His) stretch probes a subset of conformational substates with a barrier distribution comparable to that of the A-substates detected by infrared spectroscopy (Iben et al., 1989).

One comment with respect to the number of sublines used in the fitting procedure to the band shapes should be given here. Although the choice of five sublines gives good quality fits to the band shapes and supplies a physical interpretation of substates in thermodynamic equilibrium, we cannot exclude that a higher number of substates may exist. We have therefore tried to obtain good quality fits to the band shapes by use of six or seven sublines. Indeed, one obtains excellent fits of the band shapes. The thermodynamic interpretation, however, fails. The ratio $R_{ij}$ (Eq. 4) of at least two lines remains constant, completely independent of temperature. This is not in agreement with substates in thermodynamic equilibrium. Therefore, the restriction to five sublines is confirmed.

We have also performed experiments on isolated $\alpha$- and $\beta$-subunits of HbA in a 66% vol/vol glycerol/water mixture and found similar results. In the $\alpha$-subunit we found four

**TABLE 1 Peak frequencies and half-widths of the separate lines of different substates**

| | SL1 | SL2 | SL3 | SL4 | SL5 |
|---|---|---|---|---|---|
| $\Omega_i$ cm$^{-1}$ | 213 | 220 | 226 | 230.5 | 236.2 |
| $\Gamma_i$ cm$^{-1}$ | 8.1 | 8 | 8 | 7.8 | 8 |

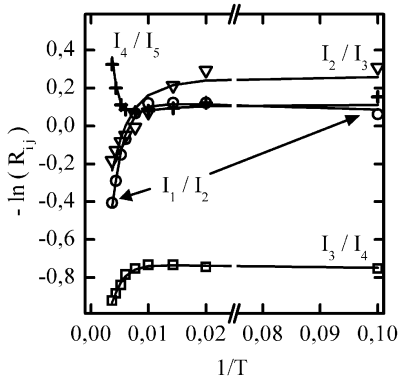


FIGURE 7 Plot of the intensity ratios $I_1/I_2$, $I_2/I_3$, $I_3/I_4$, and $I_4/I_5$ versus the reciprocal temperature $T$. The solid lines represent fits carried out by employing Eq. 4.

**TABLE 2 Fitted values for the parameters of the van 't Hoff plots**

| | $\Delta H$ (J/mol) | $\Delta S$ (J/(mol K)) | $b$ (J/(mol $K^2$)) |
|---|---|---|---|
| $I_1/I_2$ | 1610 | 10.0 | 0 |
| $I_2/I_3$ | 842 | 5.5 | 0 |
| $I_3/I_4$ | 570 | 10.0 | 0 |
| $I_4/I_5$ | 982 | 13.8 | −0.05 |

sublines for their $\nu$(Fe-His) profile and five sublines for the $\beta$-subunit. Their intensity ratios also show a van't Hoff behavior with enthalpy differences on the order of 1 kJ/mol. It should be noted here that the interpretation of the band shape of these subunits is more complex, because monomers and dimers of $\alpha$-chains as well as monomers and tetramers of $\beta$-chains coexist in solution (Valdes and Ackers, 1977). This will be reported later. It seems highly unlikely that this behavior of so many substances is accidental. Although one might argue that accompanying Raman bands that obscure the region of the of the $\nu$(Fe-His) band could give fortuitous results, this is no longer the case for the isolated band shape of sperm whale myoglobin reported here. The attempt to fit the $\nu$(Fe-His) band shapes of $\alpha$- and $\beta$-chains by the model of Bitler and Stavrov again was without success.

Taken together, the present analysis strongly confirms the notion that the $\nu$(Fe-His) band profile is determined by conformational heterogeneity. This result is in full accordance with a recent study by Peterson et al. (1998). These authors investigated the $\nu$(Fe-His) band of a variety of sw Mb mutants in which proximal amino acids such as $Leu^{89}$, $Ser^{92}$, and $His^{97}$ were substituted by other amino acids. They showed that a consistent analysis of the various $\nu$(Fe-His) bands observed requires the consideration of multiple sublines and argued that the differences in frequency values and the intensity distribution of the sublines between different mutants are not consistent with the predictions and the basic principles of an anharmonic coupling model (the authors made reference to an earlier paper by Rosenfeld and Stavrov, 1994). They provided some evidence that in contrast to earlier considerations the heterogeneity of the $\nu$(Fe-His) band reflects distributions in the azimuth angle $\phi$ of the $\nu$(Fe-His) linkage.

The earliest models of proximal linkage heterogeneity invoked a Gaussian distribution of iron out-of-plane displacement conformational substates (Šrajer et al., 1986, 1988; Steinbach et al., 1991), which can be mapped in principle onto the distribution of enthalpy barrier heights determining ligand binding. Assuming a monotonic relationship between iron displacement and $\nu$(Fe-His) frequency suggests a skew-shaped line profile for the $\nu$(Fe-His) band. Distinct structures, like shoulders, such as observed in our experiment, are in contradiction to such a model.

## CONCLUSION

The $\nu$(Fe-His) band shows a complex temperature-dependent profile, with a shoulder at its high-frequency wing. With increasing temperature, this shoulder becomes more prominent and shifts to lower frequencies. Moreover, the peak frequency decreases upon increasing temperature. This band shape was decomposed into five sublines with a common set of temperature-independent frequency positions and half-widths consistently for a set of nine band shapes at measured temperatures between 10 K and 300 K, using the line intensities as fitting parameters only. A plot of the intensity ratios $I_i/I_j$ for all sublines versus reciprocal temperature reveals a van't Hoff behavior for $T > 150$ K, with enthalpy differences on the order of 1 kJ/mol. From this behavior we conclude that each subline has to be assigned to a conformational substate of the $\nu$(Fe-His) linkage, as already suggested by Gilch et al. (1995). Above 150 K, these substates are in thermodynamic equilibrium. Below 70 K the intensity ratios of the sublines remain temperature independent, because the conformational substates are frozen below the glass transition temperature of the glycerol/water solution. Such a behavior has already been observed by Gilch et al. (1993, 1995) for horse heart deoxyMb and human deoxyhemoglobin in aqueous solutions. A similar transition temperature for the dynamics of the central iron atom was obtained from optical absorption measurements (Cupane et al., 1995).

Other arguments to explain the substates of the $\nu$(Fe-His) can be derived from the results of Franzen et al. (2000) and Kozlowski et al. (2000), who provided computational evidence that the Fe-$N_\epsilon$ stretch is vibrationally mixed with out-of-plane modes of the heme macrocycle. The work of Kozlowski et al. (2000) is particularly compelling because it is based on high-level density functional theory calculations that reproduced the spin state of the pentacoordinated heme-imidazole complex. Their results strongly suggest that $\nu$(Fe-His) is in fact a mixture of the Fe-imidazole stretch and the $A_{2u}$-type out-of-plane mode $\gamma_9$. It is conceivable that the degree of this mixing depends on the doming distortion of the heme group, which is likely to cause additional mixing with in-plane modes ($\nu_9$) of the heme group (Unger et al., 1999). Thus, one can invoke a mapping of different conformational substates of the doming distortions onto the $\nu$(Fe-His) frequency within the framework of the harmonic approximation, in contrast to the basic assumption of Bitler and Stavrov (1999).

Our results clearly exclude the conclusion drawn by Bitler and Stavrov (1999) that the $\nu$(Fe-His) band shape can be accounted for exclusively by anharmonic coupling of the vibration of a uniquely defined $\nu$(Fe-His) linkage with a low-frequency out-of-plane vibration of Fe in the porphyrin skeleton. For sw deoxyMb, it turns out that it is practically impossible to fit the band shape by the anharmonic coupling model.

It should be finally mentioned that the anharmonic coupling mechanism cannot be refused entirely. If it exists, it would change the line shape of each subline as suggested by Bitler and Stavrov. A fit combining both models, however, might be possible but needs many more parameters and therefore will not be convincing and unique.

In conclusion, we contradict the final statement of Bitler and Stavrov (1999) for an exclusion of substates. Our results clearly prove the existence of taxonomic substates in the $Fe^{2+}$-$N_\epsilon(His^{F8})$ linkage in heme-proteins.

We thank Dr. A. Ostermann and Prof. Dr. F. G. Parak for supplying the $^{54}Fe$ sample. We are grateful to J. Lauckner for excellent technical support. This work is supported by a grant from the Deutsche Forschungsgemeinschaft.

## REFERENCES

Ansari, A., J. Berendzen, S. F. D. Braunstein, B. R. Cowen, H. Frauenfelder, M. K. Kong, I. E. T. Iben, J. B. Johnson, P. Ormos, T. B. Sauke, R. Scholl, A. Schulte, P. J. Steinbach, J. Vittitow, and R. D. Young. 1987. Rebinding and relaxation in the heme pocket. *Biophys. Chem.* 26:337–355.

Argade, P. V., M. Sassaroli, D. L. Rousseau, T. Inubushi, M. Ikeda-Saito, and A. Lapidot. 1984. Confirmation of the assignment of the iron-histidine stretching mode in myoglobin. *J. Am. Chem. Soc*. 106: 6593–6596.

Bitler, A., and S. S. Stavrov. 1999. Iron-histidine resonance Raman band of deoxyheme proteins: effects of anharmonic coupling and glass-liquid phase transition. *Biophys. J.* 77:2764–2776.

Bosenbeck, M., R. Schweitzer-Stenner, and W. Dreybrodt. 1992. pH induced conformational changes of $Fe^{2+}$-$N_\epsilon$(His F8) linkage in deoxyhemoglobin trout IV detected be the Raman active $Fe^{2+}$-$N_\epsilon$(His F8) stretching mode. *Biophys. J.* 61:31–41.

Braunstein, D. P., K. Chu, K. D. Egeberg, H. Frauenfelder, J. R. Mourant, G. U. Nienhaus, P. Ormos, S. G. Sligar, B. A. Springer, and R. D. Young. 1993. Ligand binding to heme proteins. III: FTIR studies of His-E7 and Val-E11 mutants of carbonmonoxymyoglobin. *Biophys. J.* 65:2447–2454.

Cupane, A., M. Leone, E. Vitrano, and L. Cordone. 1995. Low temperature optical absorption spectroscopy. An approach to study stereodynamic properties of hemeproteins. *Eur. Biophys. J.* 23:385–398.

Doster, W., S. Cusack, and W. Petry. 1989. Dynamic transitions of myoglobin revealed by inelastic neutron scattering. *Nature.* 337:754–756.

Franzen, S., S. G. Boxer, R. B. Dyer, and W. H. Woodruff. 2000. Resonance Raman studies of heme axial ligation in H93G myoglobin. *J. Phys. Chem. B.* 104:10359–10367.

Frauenfelder, H., S. S. Sligar, and P. G. Wolynes. 1991. The energy landscape and motions of proteins. *Science.* 254:1598–1603.

Friedman, J. 1985. Structure, dynamics and reactivity in hemoglobin. *Science.* 228:1274–1280

Gellin, B. R., A. W.-M. Lee, and M. Karplus. 1983. Hemoglobin tertiary structure change on ligand binding. Its role in the co-operative mechanism. *J. Mol. Biol.* 171:489–559.

Gilch, H., W. Dreybrodt, and R. Schweitzer-Stenner. 1995. Thermal fluctuations between conformational substates of the $Fe^{2+}$-$N_\epsilon(His^{F8})$ linkage in deoxymyoglobin probed by the Raman active Fe- $N_\epsilon(His^{F8})$ stretching vibration. *Biophys. J.* 69:214–227.

Gilch, H., R. Schweitzer-Stenner, and W. Dreybrodt. 1993. Structural heterogeneity of the $Fe^{2+}$-$N_\epsilon(His^{F8})$ bond in various hemoglobin and myoglobin derivatives probed by the Raman active iron histidin stretching mode. *Biophys. J.* 65:1470–1485.

Gilch, H., R. Schweitzer-Stenner, W. Dreybrodt, M. Leone, A. Cupane, and L. Cordone. 1996. Conformational substates of the $Fe^{2+}$-His F8 linkage in deoxymyoglobin and hemoglobin probed in parallel by the Raman band of the Fe-His stretching vibration and the near-infrared absorption band III. *Int. J. Quant. Chem.* 59:301–313.

Hori, H., and T. Kitagawa. 1980. Iron-ligand stretching band in the resonance Raman spectra of ferrous iron porphyrin derivatives. Importance as a probe band for quarternary structure of hemoglobin. *J. Am. Chem. Soc.* 102:3608–3613.

Iben, I. E. T., D. Braunstein, W. Doster, H. Frauenfelder, M. K. Hong, J. B. Johnson, S. Luck, P. Ormos, A. Schulte, P. J. Steinbach, A. H. Xie, and R. D. Young. 1989. Glassy behavior of a protein. *Phys. Rev. Lett*. 62:1916–1919.

Kitagawa, T. 1988. The heme protein structure and the iron histidine stretching mode. *In* Biological Application on Raman Spectroscopy. T.G. Spiro, editor. John Wiley and Sons, New York. 97–131.

Kitagawa, T., K. Nagai, and M. Tsubaki. 1979. Assignment of the Fe-$N_\epsilon$ (HisF8) stretching band in the resonance Raman spectra of deoxy myoglobin, *FEBS Lett*. 104:376–378.

Kozlowski, P., T. G. Spiro, and M. Z. Zgierski. 2000. DFT study of structure and vibrations in low-lying spin states of five-coordinated deoxyheme model. *J. Phys. Chem. B.* 104:10659–10666.

Parak, F., E. W. Knapp, and D. Kucheida. 1982. Protein dynamics. Mössbauer spectroscopy on deoxymyoglobin crystals. *J. Mol. Biol*. 161: 177–194.

Peterson, E. S., J. M. Friedman, Y. T. Chien Ellen, and S. G. Sligar. 1998. Functional implications of the proximal hydrogen-bonding network in myoglobin: a resonance Raman and kinetic study of Leu89, Ser92, His97, and F-helix swap mutants. *Biochemistry* 37:12301–12319.

Rosenfeld, Y. B., and S. S. Stavrov. 1994. Anharmonic coupling of soft modes and its influence on the shape of the iron-histidine resonance Raman band of heme proteins. *Chem. Phys. Lett.* 229:457–464.

Rousseau, D. L., and J. M. Friedman. 1988. Transient and cryogenic studies of photodissociated hemoglobin and myoglobin. *In* Biological Application on Raman Spectroscopy. T.G. Spiro, editor. John Wiley and Sons, New York. 133–216.

Šrajer, V., L. Reinisch, and P. M. Champion. 1988. Protein fluctuations, distribution coupling, and the binding of ligands to heme proteins. *J. Am. Chem. Soc.* 110:6656–6670.

Šrajer V., K. T. Schomacker, and P. M. Champion. 1986. Spectral broadening in biomolecules. *Phys. Rev. Lett*. 57:1267–1270.

Steinbach, P. J., A. Ansari, J. Berendzen, D. Braunstein, K. Chu, B. R. Cowen, D. Ehrenstein, H. Frauenfelder, J. B. Johnson, D. C. Lamb, S. Luck, J. R. Mourant, G. U. Nienhaus, P. Ormos, R. Philipp, A. Xie, and R. D. Young. 1991. Ligand binding to heme proteins: connection between dynamics and function. *Biochemistry.* 30:3988–4001.

Teale, F. W. J. 1959. Cleavage of the haem-protein link by acid methylethylketon. *Biochim. Biophys. Acta.* 35:543.

Unger, E., M. Beck, R. J. Lipski, W. Dreybrodt, C. J. Medforth, K. M. Smith, and R. Schweitzer-Stenner. 1999. A new method for evaluating the conformations and normal modes with a reduced force field. 2. Application to nonplanar distorted metal porphyrins. *J. Phys. Chem. B.* 103:10022–10031.

Unger, E., W. Dreybrodt, and R. Schweitzer-Stenner. 1997. Conformational properties of nickel(II)-*meso*-tetraphenylporphyrin in solution. Raman dispersion spectroscopy reveals the symmetry of distortions for a nonplanar conformer. *J. Phys. Chem*. A, 101:5997–6007.

Valdes, R., Jr., and G. K. Ackers. 1977. Thermodynamic studies on subunit assembly in human hemoglobin. *J. Biol. Chem.* 252:74–81.